Finite-Control-Set Model Predictive Control to Suppress Oscillations in Inductive Power Transfer Systems with Constant Voltage Load

Zeinab Karami*, Giuseppe Guidi†, Jon Are Suul*†

*Department of Engineering Cybernetics, *Norwegian University of Science and Technology,* Trondheim, Norway
†*SINTEF Energy Research,*.
zeinab.k.h.abadi@ntnu.no, Giuseppe.Guidi@sintef.no, jon.are.suul@ntnu.no

***Abstract*—This paper presents a finite-control-set model predictive control (FCS-MPC) strategy for pulse density modulation (PDM) in inductive power transfer (IPT) systems. The main purpose of this method is to suppress current/power ripples while ensuring high efficiency and fast dynamic response. The proposed control method is based on a nonlinear model of the IPT system when charging a battery appearing as a constant voltage load (CVL) and considers all the possible switching states for each period within the control horizon. The switching states are obtained based on optimal decision variables at each sampling time which provide the minimum value of the cost function. This results in the skipping of voltage pulses, which ensures that zero voltage switching (ZVS) occurs over the full range of operation. Moreover, by predicting the future behaviour of the studied system, the proposed control method will inherently suppress oscillations that can be excited by the skipped voltage. As a result, the system's performance is improved with respect to high efficiency and fast dynamic response. The effectiveness and performance of the proposed control method are verified by the simulation results.**

***Index Terms*—Constant voltage load, finite-control-set model predictive control, inductive power transfer, suppress oscillations.**

I. Introduction

Inductive power transfer (IPT) technologies are becoming increasingly popular for various applications such as mobile devices, marine transportation, and electric vehicles (EVs) [1]. This technology offers several advantages over traditional wired charging methods, including significant flexibility, convenience, high reliability, and the capability of becoming fully automated without the necessity of lengthy and expensive cabling [1], [2]. However, to achieve maximum efficiency, IPT systems must be able to ensure soft switching with controllable power transfer over the full required operating range. In high-power transport applications, this can be challenging under highly variable conditions such as a large changes in coupling and output power. Therefore, in order to guarantee optimal efficiency and fast dynamic response during power transfer using model-based control methods, an accurate dynamic model of the system is essential.

This work was supported by the Research Council of Norway (RCN) under Project number 304213, "Research and Demonstration of Key Technologies for Intelligent-connected Electric Vehicles in China and Norway" ("KeyTech NeVeChiNo).

For high-power battery charging applications series-series (SS)-compensated IPT systems with a diode-rectifier on receiving side are often most suitable. In such systems, the receiving side diode rectifier allows for minimizing the number of components, costs, and losses, but implies that the system must be fully controlled from the sending side. [3]. In the previous literature, IPT systems are usually modelled with a constant-resistance load (CRL) [4], [5]. However, this model is not adequate for the dynamic analysis and control system design of battery charging systems. Instead, a constant voltage load (CVL) can be used to represent the practical condition of a battery connected directly to the rectifier terminals on the receiving side [6].

Modulator based control methods such as phase-shift modulation (PSM) is the most common technique for power control and voltage regulation among control methods in IPT charging systems [7]. However, this technique results in increased losses and reduced system efficiency at low output voltage due to the hard switching. To overcome this challenge, pulse skipping modulation such as pulse density modulation (PDM) [8] and ON-OFF keying (OOK) modulation [9] are used in such systems to accomplish soft switching in the full operating range. These methods can always achieve zero voltage switching (ZVS) under different power conditions by skipping pulses for adjusting the average sending voltage. However, these methods can excite a poorly damped oscillation mode in IPT systems with CVLs, which can result in high current/power ripples [10]. To solve this problem, an active damping method to attenuate the oscillations caused by the skipped pulses of the PDM is presented in [10]. However, the active damping method transiently introduces a PSM, which implies hard switching and increased losses.

Model predictive control (MPC) methods are widely investigated for power electronic applications due to significant increase in the computing power of microprocessors, which can perform the large amount of calculations with high speed and lower cost [11]. Recently, these methods have been used for IPT charging systems to improve the dynamic response of power control and voltage regulation [12]–[14]. MPC is an optimal control method that aims to solve an optimization problem over a prediction horizon at each sampling step. There are several advantages of using this technology, including fast

dynamic response, consideration of non-linearity dynamics, uncertainty, and constraints of state variables and input variables [11]. Generally, MPC is divided into two categories: continuous control set MPC (CCS-MPC) and finite control set MPC (FCS-MPC). The CCS-MPC calculates a continuous control signal and then uses a modulator to generate the output voltage of the converter [15]. In contrast the FCS-MPC is able to consider switching behaviour in control algorithm, which leads to a decrease of delay between the control and actuation stages due to avoiding the need for modulators [16].

This paper proposes an FCS-MPC implementation for IPT-based EV charging systems by considering a nonlinear dynamic model of CVL for power flow control and ripple reduction. In contrast to the PI-based control methods, the proposed FCS-MPC strategy provides a faster dynamic response and can effectively overcome the effects of disturbances, and nonlinearities, while reducing the current/power ripples [10]. The proposed method can guarantee efficiency and power regulation by considering the nonlinear dynamic model of the system in the presence of CVL, which has been ignored in previous MPC-based control methods for IPT charging system in [13]–[15]. Furthermore, the modulators such as PSM, PDM, etc., have been used in these papers to achieve the switching sequences for power converters [13], [17]. As opposed to the previous methods, the proposed FCS-MPC control method avoids the delay between the control and modulator stage by considering the switching characteristic in the control algorithm. Moreover, compared to the first FCS-MPC proposal for an IPT charging system with CVL in [16], the presented implementation in this paper does not require a low-pass filter (LPF) in the feedback control loop to prevent large current/power ripples.

The main purpose of the proposed control method is to regulate the power transfer, while minimizing the current/power fluctuations by determining the optimal control signals. In this regard, the FCS-MPC approach utilizes a prediction model to estimate future system behavior, including state variables and output power. Therefore, current/power ripples are inherently suppressed by minimizing a multi-objective cost function, defined as the difference between predicted and reference values at each sampling instance. Furthermore, the proposed control method can guarantee the soft switching performance by skipping of the voltage pulses, while maintaining high efficiency with fast dynamic response. The confirmation and performance of the proposed FCS-MPC control method for IPT system with CVL by considering different cost functions in control algorithm is validated by simulation results. In this regard the proposed FCS-MPC control method with/without the damping term is evaluated and compared to suppress current/power ripples.

II. CONFIGURATION OF IPT SYSTEM WITH CVL

Fig. 1(a) shows the electric circuit of the SS-compensated IPT charging system with CVL. The equivalent circuit of such system with both CRL and CVL modes is illustrated in Fig. 1(b). As can be seen, it consists of a high-frequency full bridge

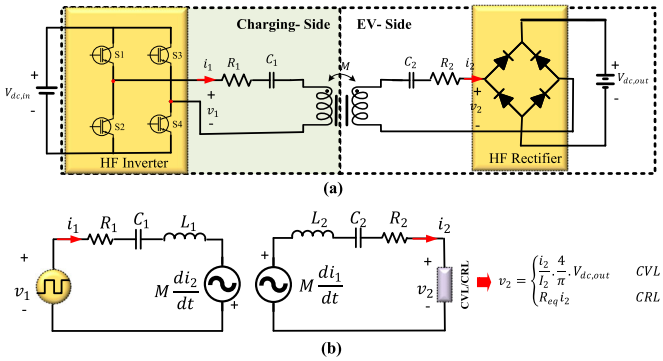

Fig. 1. (a) Schematic diagram of SS-compensated IPT charging system with CVL, (b) Equivalent circuits using fundamental harmonic approximation with CVL or CRL.

inverter with a constant dc voltage source as input voltage $V_{dc,in}$ on the primary side. i_1, i_2, v_1 and v_2 are defined as the sending/pickup currents and voltages, respectively. R_1, C_1, L_1, and R_2, C_2, L_2 are series equivalent resistance, capacitance and inductance of primary and secondary coils, respectively, and M is the mutual inductance between two coils.

According to the first harmonic approximation in a synchronously rotating dq reference frame, the non-linear state-space model of the SS-compensated IPT system with CVL can be referred to [3]. This model can be given by:

$$\dot{x} = f(x,u) \tag{1}$$
$$y = g(x,u) \tag{2}$$

where $f(x,u)$ can be represented as follows:

$$\begin{aligned}
\dot{x}_1 &= -\frac{R_1}{L_{\alpha1}}\cdot x_1 + \omega\cdot x_2 - \frac{MR_2}{L_{\alpha1}L_2}\cdot x_3 - \frac{1}{L_{\alpha1}}\cdot x_5 \\
&\quad -\frac{M}{L_{\alpha1}L_2}\cdot x_7 + \frac{1}{L_{\alpha1}}\cdot v_{1,d} - \frac{M}{L_{\alpha1}L_2}\cdot v_{2,d} \\
\dot{x}_2 &= -\omega\cdot x_1 - \frac{R_1}{L_{\alpha1}}\cdot x_2 - \frac{MR_2}{L_{\alpha1}L_2}\cdot x_4 - \frac{1}{L_{\alpha1}}\cdot x_6 \\
&\quad -\frac{M}{L_{\alpha1}L_2}\cdot x_8 + \frac{1}{L_{\alpha1}}\cdot v_{1,q} - \frac{M}{L_{\alpha1}L_2}\cdot v_{2,q} \\
\dot{x}_3 &= -\frac{MR_1}{L_{\alpha2}L_1}\cdot x_1 - \frac{R_2}{L_{\alpha2}}\cdot x_3 + \omega\cdot x_4 - \frac{M}{L_{\alpha2}L_1}\cdot x_5 \\
&\quad -\frac{1}{L_{\alpha2}}\cdot x_7 + \frac{M}{L_{\alpha2}L_1}\cdot v_{1,d} - \frac{1}{L_{\alpha2}}\cdot v_{2,d} \\
\dot{x}_4 &= -\frac{MR_1}{L_{\alpha2}L_1}\cdot x_2 - \omega\cdot x_3 - \frac{R_2}{L_{\alpha2}}\cdot x_4 - \frac{M}{L_{\alpha2}L_1}\cdot x_6 \\
&\quad -\frac{1}{L_{\alpha2}}\cdot x_8 + \frac{M}{L_{\alpha2}L_1}\cdot v_{1,q} - \frac{1}{L_{\alpha2}}\cdot v_{2,q} \\
\dot{x}_5 &= \frac{1}{C_1}\cdot x_1 + \omega\cdot x_6, \qquad \dot{x}_6 = \frac{1}{C_1}\cdot x_2 - \omega\cdot x_5 \\
\dot{x}_7 &= \frac{1}{C_2}\cdot x_3 + \omega\cdot x_8, \qquad \dot{x}_8 = \frac{1}{C_2}\cdot x_4 - \omega\cdot x_7
\end{aligned} \tag{3}$$

where $x = [i_{1,d}\ i_{1,q}\ i_{2,d}\ i_{2,q}\ v_{c1,d}\ v_{c1,q}\ v_{c2,d}\ v_{c2,q}]^T$ is state variable in dq model, $u = [v_{1,d}\ \ v_{1,q}]^T$ is output voltage of the full-bridge (FB) inverter on the primary-side as control

signal. By aligning the voltage vector to the d axis, the output voltage of the q channel $v_{1,q} = 0$. Therefore, the input control signal is simplified as $u = v_{1,d}$. $L_{\alpha 1} = L_1 - M^2/L_2$ and $L_{\alpha 2} = L_2 - M^2/L_1$ are leakage inductance of sending/pickup sides. Furthermore, to achieve the maximum coil-to-coil efficiency in the IPT systems, the operating angular frequency ω should be equal to the resonant angular frequency ω_0 [18], where $\omega_0 = 2\pi f_0$, and f_0 is resonance frequency which should satisfy $f_0 = 1/2\pi\sqrt{L_1C_1} = 1/2\pi\sqrt{L_2C_2}$. $v_{2,d}$ and $v_{2,q}$ are dq-components of the pickup voltage which is different for the CRL and CVL models [10]. The nonlinear term associated with the CVL characteristics of the studied IPT system can be defined by (4), where $V_{dc,out}$ is expressed as the dc output voltage value.

$$v_{2,dq} = \frac{4}{\pi} \cdot V_{dc,out} \cdot \frac{i_{2,dq}}{\sqrt{i_{2,d}^2 + i_{2,q}^2}} \tag{4}$$

Furthermore, the output power P_{out} is considered as the output signal (i.e, y), which in dq reference frame can be calculated as:

$$P_{out} = V_{2,d}.i_{2,d} + V_{2,q}.i_{2,q} = \frac{4}{\pi}.V_{dc,out}.\frac{i_{2,d}^2 + i_{2,q}^2}{\sqrt{i_{2,d}^2 + i_{2,q}^2}} \tag{5}$$

III. Proposed Control System Design

A design and implementation of the FCS-MPC method for power control and elimination of oscillations in an IPT system with CVL is presented in this section. A schematic overview of the proposed FCS-MPC control method for the studied system is shown in Fig. 2. To calculate the proposed FCS-MPC control commands, as a first step, the future behaviour of the system will be predicted based on the measured/estimated values of the inductor currents and capacitor voltages on both sides in the current sample k (i.e., $x(k)$). In this regard, a discrete-time form of the continuous-time dynamic model of the system from (3) for a sampling time (T_s) with the measured/estimated values at the present discrete sampling instant (k) is used. The derivative of system as a discrete-time model can be approximated by the forward Euler approach as follows:

$$\frac{dx(t)}{dt} = \frac{x(k+1) - x(k)}{T_s} \tag{6}$$

The nonlinear state-space representation of the system based on an average discrete-time model can be represented as follows:

$$x(k+1) = x(k) + T_s f(x(k), u(k)) \tag{7}$$

where $x(k)$ and $x(k+1)$ are defined as the state vectors at k and $(k+1)$ instants (previous and predicted values), respectively. $k = nT_s, n \in Z^+$ is sample instant, and $T_s = 1/(2f_0)$ is the sampling time of the MPC controller. $u(k)$ is control signal, which is d-axis of the output voltage of the FB inverter on the primary-side. It can be defined as $v_{1,d}(k) = U \cdot \frac{4}{\pi} \cdot V_{dc,in}$ where $U \in \{-1, 0, 1\}$ to be consistent with the discrete nature of the inverter as finite control decision

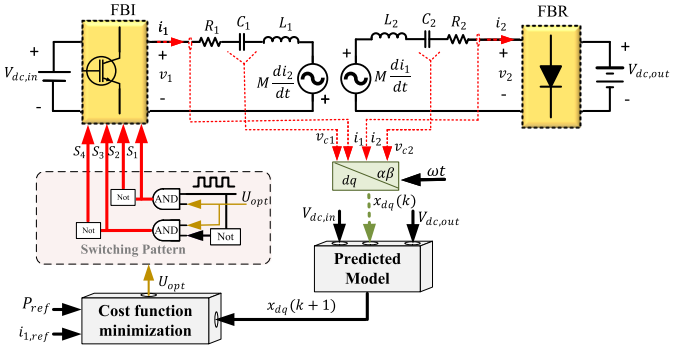

Fig. 2. The block diagram of the proposed FCS-MPC control method.

variables. According to this explanation, the nonlinear average discrete-time model of system in (7) can be rewritten by:

$$x(k+1) = \begin{cases} x(k) + T_s f(x(k)) & U = 0 \\ x(k) + T_s f(x(k), v_{1,d}(k)) & U = 1 \quad or \quad -1 \end{cases} \tag{8}$$

In the second step of the proposed control design, the predicted values $x(k+1)$ and the reference values (P_{ref} and $i_{1,ref}$) are selected as a cost function based on control objective. The cost function is calculated to achieve the control objectives (power tracking and oscillation reduction). This control design is primarily intended to achieve minimum tracking errors. In this regard, a preliminary cost function is proposed in equation (9) with the only purpose of regulating the output power (P_{out}) to the reference power (P_{ref}) to achieve a minimum power tracking error.

$$J_1(k) = \left(P_{out}^p(k+1) - P_{ref}\right)^2 \tag{9}$$

where P_{ref} and $P_{out}^p(k+1)$ are output reference and predicted power, respectively. The predicted output power of IPT system with CVL is calculated as:

$$P_{out}^p(k+1) = \frac{4}{\pi} V_{dc,out} \frac{(i_{2,d}^p(k+1))^2 + i_{2,d}^p(k+1))^2}{\sqrt{(i_{2,d}^p(k+1))^2 + (i_{2,q}^p(k+1))^2}} \tag{10}$$

As shown in Fig. 3, by using the cost function (J_1), the proposed FCS-MPC can track the power reference with fast response, but there can still occur current/power ripple. Therefore, to address this issue, a multi-objective cost function consisting of two weighted terms is defined as given by (11). It can be seen that by adding the damping term, the proposed FCS-MPC can significantly reduce the current/power ripple while retaining high performance and fast dynamic response.

$$J_{tot}(k) = \lambda_1 J_1 + \lambda_2 J_2 \tag{11}$$

To demonstrate the exact performance of these two objectives, the first objective J_1 represents power tracking by measuring the difference between the predicted output power and its reference value. The second objective (J_2) is responsible for suppressing current/power oscillations as a damping term,

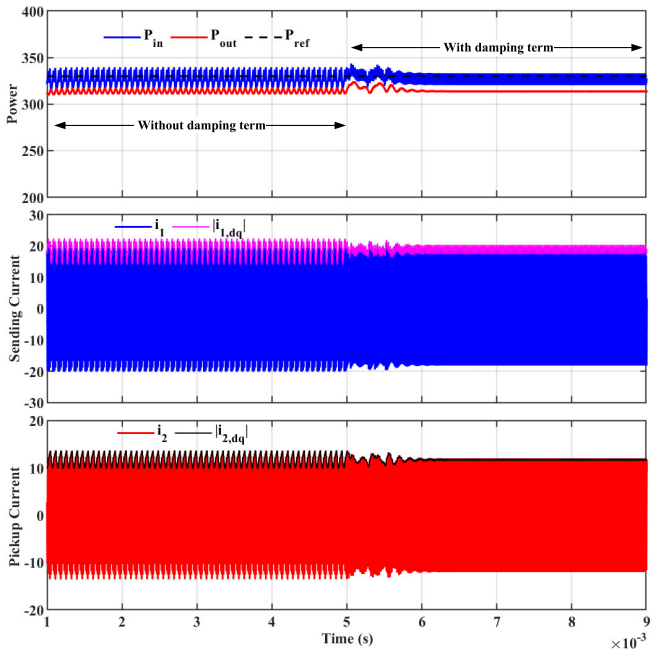

Fig. 3. Performance of the IPT system using the proposed FCS-MPC with different cost function.

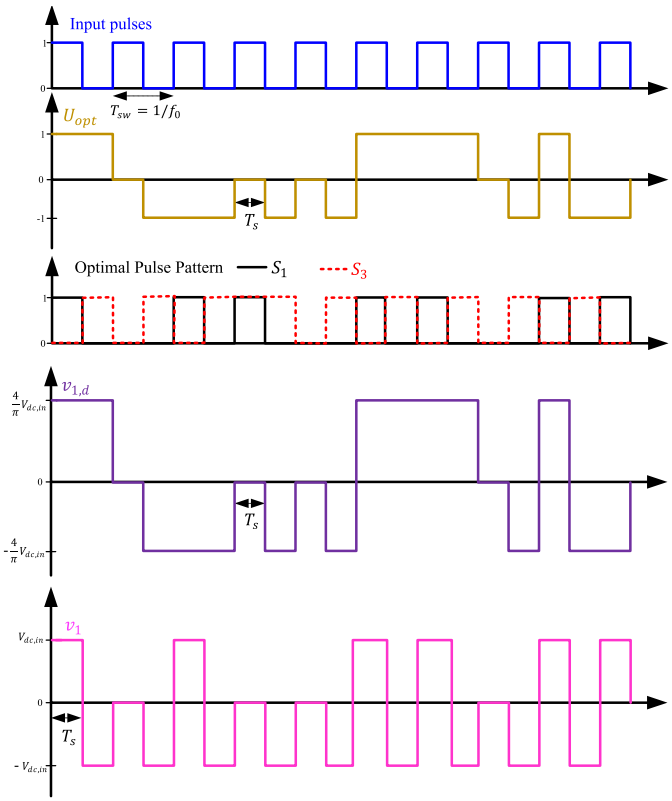

Fig. 4. Control signal waveform using the proposed FCS-MPC.

which is calculated by $J_2 = (i_1^p(k+1) - i_{1,ref})^2$; therefore, the total cost function can be rewritten as follows:

$$J_{tot}(k) = \lambda_1 \left(P_{out}^p(k+1) - P_{ref}\right)^2 + \lambda_2 \left(i_1^p(k+1) - i_{1,ref}\right)^2 \tag{12}$$

where λ_1 and λ_2 are the weighting factors which represent the deviation and damping terms, respectively. The weighting factor is used to balance control objectives and constraints that affect the performance of the proposed control method. It is not easy to determine the appropriate weighting factors in order to achieve the desired behaviour of a system. In fact, to obtain the value of weighting factor, several factors must be taken into account, such as the peak value, settling time, oscillation magnitude, etc. In this paper, the trial and error method is used to obtain the appropriate weighting factor. In this way, figures of merit are defined depending on the application, and a series of simulations are performed to find the most appropriate value [20]. Moreover, $i_1^p(k+1)$ and $i_{1,ref}$ are predicted and reference values of sending current, respectively which can be expressed by:

$$i_1^p(k+1) = \sqrt{(i_{1,d}^p(k+1))^2 + (i_{1,q}^p(k+1))^2} \tag{13}$$

$$i_{1,ref} = \frac{P_{ref}}{V_{1,nom}} \tag{14}$$

where $V_{1,nom}$ is nominal value of sending voltage and $i_{1,dq}^p(k+1)$ is defined as dq-components of the predicted sending current.

Finally, the optimization problem is used to find the optimal values of the decision variables that will minimize the cost function and achieve the desired objectives (e.g., $v_{1,d}$). To achieve accurate control of the power transfer and suppress the power/current ripple, it is necessary to obtain the optimal control sequence at each sampling time over prediction horizon, which is achieved by solving the cost function subject to constraints imposed by the system. In light of this, the output of the proposed FCS-MPC is the result of the local optimization problem. Hence, the value of U_{opt} in Fig. 2 can be determined by minimizing the cost function at each sampling time (i.e. a half cycle $T_s = 0.5T_{sw}$), which is expressed as follows:

$$U_{opt}(k) = \arg\min J_{tot}(k) \tag{15}$$

$$\text{subject to:} \quad Eq(1) - (7),$$
$$i_{1,min} \le i_1 \le i_{1,max}, i_{2,min} \le i_2 \le i_{2,max}$$
$$\text{and} \quad U_{opt} \in \{-1, 0, 1\}$$

So that at any sample time the minimum index k which represents minimum J_{tot} is found and $U_{opt}(k) = \{u^*(k), u^*(k+1), ...\}$ is considered as the output of the optimization problem. There exist 3^N voltage sequences and only its first element i.e., $u^*(k)$ is applied to the pulse pattern at each sampling time. Then the prediction horizon is shifted one step forward, and these steps are repeated each sample time with updated measurements or estimations.

Fig. 4 shows an example of a control signal waveform using the proposed FCS-MPC. As can be seen, the optimal control decision variable $U_{opt} \in \{-1, 0, 1\}$ is selected at

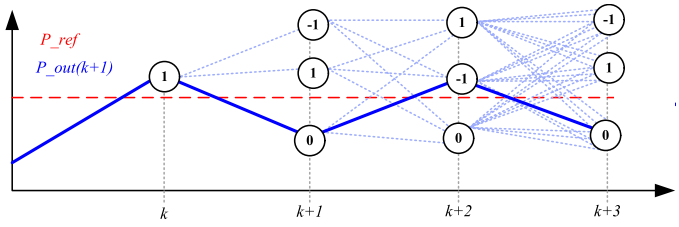

Fig. 5. The operating principle of the proposed FCS-MPC (steady-state).

each sampling time. Then, based on the positive, negative and skipping pulse operations, the value of $v_{1,d}$ equals the peak value of the first harmonic approximation of the input voltage or zero. When the optimal decision variable is selected as $U_{opt} = 1$, the reference square wave signal is applied to each leg of the FB inverter v_1 (corresponding to $v_{1,d} = 4/\pi \cdot V_{dc,in}$ and independent of whether it is in the positive or negative half cycle). If $U_{opt} = -1$, the opposite voltage to the reference square wave signal (i.e. related to $v_{1,d} = -4/\pi \cdot V_{dc,in}$ and independent of whether it is in the positive or negative half cycle) will be applied. Otherwise, zero voltage will be applied if U_{opt} equal to zero leads to the minimization of the cost function. Furthermore, the operating principle of the proposed FCS-MPC is illustrated in Fig. 5. It can be seen that the manipulated variables are {-1,0,1} as all possible solutions. At each time step, the states are computed then the cost function is evaluated for each of these voltage vectors, and finally, the one decision variable that has the smallest cost value is selected. Normally, all possible combinations should be considered to find the optimal control signal (i.e., U_{opt}). In this regard, there are three different combinations from time step k to $k+1$ and at the next time step 3^2. It can be stated that the number of possible combinations increases exponentially with N (3^N). Therefore, in this paper, N is set equal to one in order to avoid a high computational burden.

IV. Simulation Results

In section III, a multi-objective cost function has been presented to suppress oscillations caused by CVL characteristics. A trade-off between oscillation damping and steady-state error should be considered, which can be addressed by tuning weighting factors λ_1 and λ_2. This method can ensure the system performance with very low current/power ripple, high efficiency and fast dynamic response. To validate the effectiveness of the proposed FCS-MPC method for SS-compensated IPT systems with CVL, simulations have been conducted with a model in Matlab/Simulink. The parameters of the proposed IPT system are provided in Table I.

Fig. 6 shows the performance of the studied IPT system using the proposed FCS-MPC method when operated in steady-state performance at $0.75P_{nom}$. As can be seen the proposed control method can eliminate current/power ripple of the IPT system. The result of the IPT system with proposed control method by considering the total cost function (J_{tot}) is shown in Fig. 6(b). In comparison to Fig. 6(a), in which the control algorithm only used the standard power tracking cost function (J_1), current/power oscillations have been greatly reduced. It can be verified based on the peak-to-peak sending current, which has been reduced to $36.8A$ through the proposed control method with damping term compared to $40.2A$ in case without damping term. Indeed, as shown in Fig. 6(a), the proposed control method with only tracking cost function (J_1) does not provide an accurate response and has a large power/current ripple due to a poorly damped oscillation mode of IPT systems with CVL. However, these power and current fluctuations can be significantly reduced by adding the damping term (J_2) in the total cost function (J_{tot}) and adjusting the weighting factors (see Fig. 6(b)). Furthermore, to validate the ZVS performance of the IPT system using the proposed FCS-MPC, the closed-loop system is tested under different power variations as seen in Fig. 7. It can be verified that the IPT system using FCS-MPC always achieves soft switching conditions, while ensuring low switching losses and thereby high efficiency.

Additionally, to confirm the dynamic performance of the proposed FCS-MPC, the response to a change of the power reference is presented. Fig. 8 shows a comparison of the dynamic response of the power transfer and sending/pickup current using the proposed FCS-MPC control methods under reference power change in the system without/with damping term (i.e, second cost function (J_2)). It is assumed that a step change in the reference power is imposed from the initial value of $P_{ref} = 0.6P_{nom}$ to $P_{ref} = 0.75P_{nom}$ at $t = 5ms$. It can be seen that in both cases, the transferred power reaches steady-state very quickly, after only $0.5ms$. However, the proposed control method without a damping term produces a large current/power fluctuations. By adding the damping term in the conventional MPC method and using a multi-objective cost function, the FCS-MPC can reach the steady-state and significantly suppress oscillations. As the results indicate, the transferred power of the system utilizing the proposed FCS-MPC with the damping term is smoother than that of the system using the proposed FCS-MPC without the damping term. Moreover, the maximum sending current amplitude of the undamped system has fluctuation compared to the system with the added cost function J_2 which remains stable throughout the entire process. Thus, the proposed FCS-MPC based on a multi-objective cost function can effectively suppress current/power ripples in any situation.

As previously mentioned, the nonlinear state-space model of the IPT system with CVL is derived by first harmonic ap-

TABLE I
Electrical and Control Parameters.

Electrical Parameters of the IPT system		
Parameter	**Symbol**	**Value**
Nominal Power	P_{nom}	440 W
Nominal Sending Voltage	$V_{,nom1}$	52 V
Nominal Receiving Voltage	$V_{2,nom}$	50 V
Nominal Coupling Coefficient	k_c	0.18
Resonance Frequency	f_0	85 kHz
Primary/Secondary self inductances	L_1/L_2	31.24/30.85 μH
Primary/Secondary capacitances	C_1/C_2	117.83/113.64 μF
Primary/Secondary Resistances	R_1/R_2	0.0525/0.0555 Ω
Detuning factor	x_c	1.05

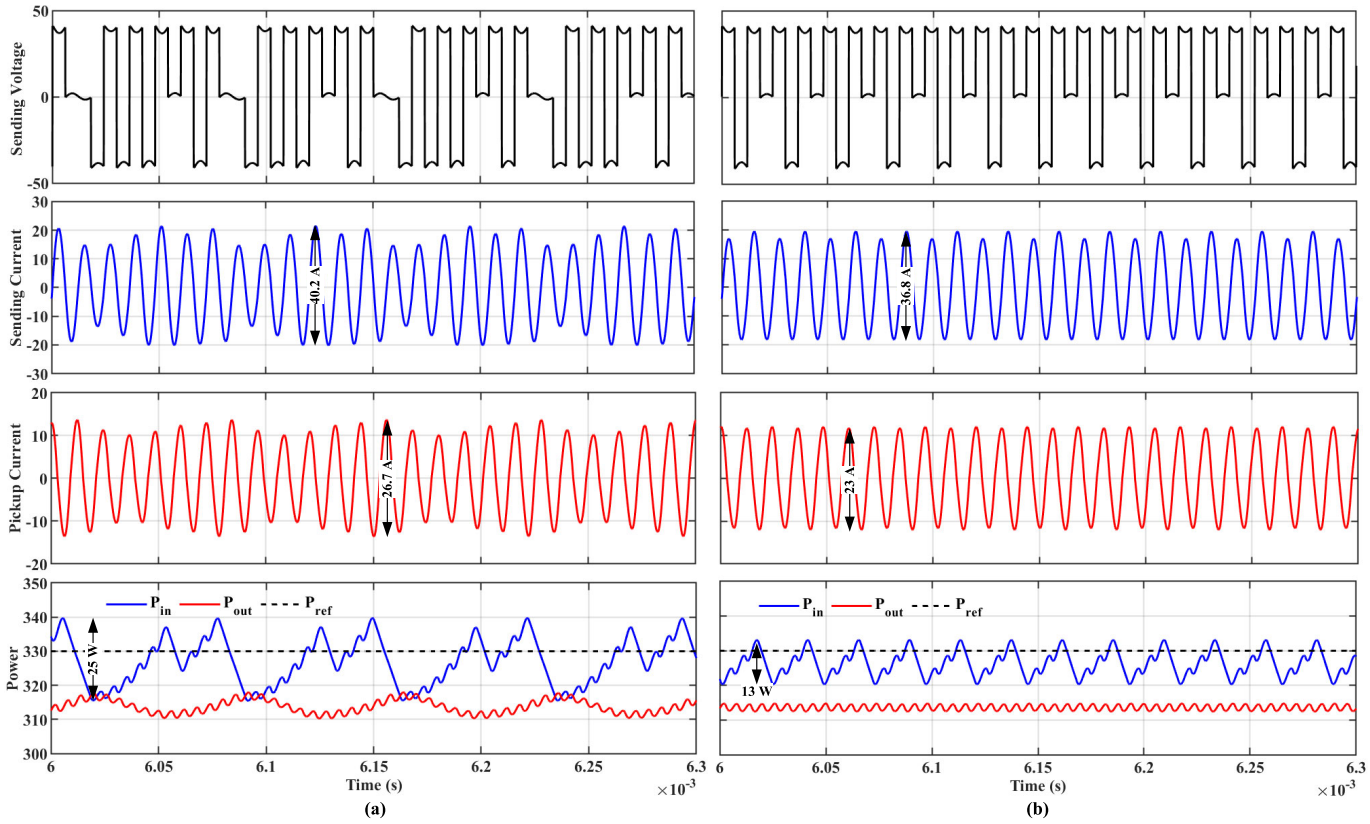

Fig. 6. Steady-state performance of the IPT system using the proposed FCS-MPC at $P_{ref} = 0.75P_{nom}$: (a) with the cost function J_1, (b) with total cost function J_{tot}.

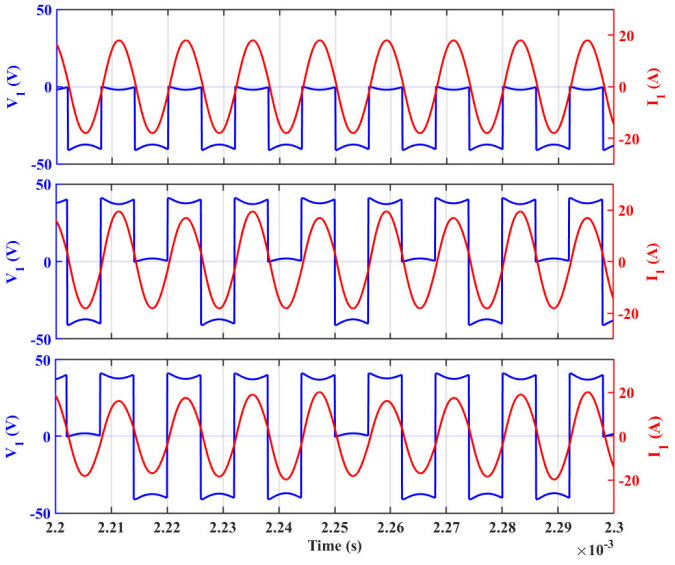

Fig. 7. ZVS operation of the IPT system using the proposed FCS-MPC under different power: (a) $0.5P_{nom}$, (b) $0.75P_{nom}$ and (c) $0.875P_{nom}$.

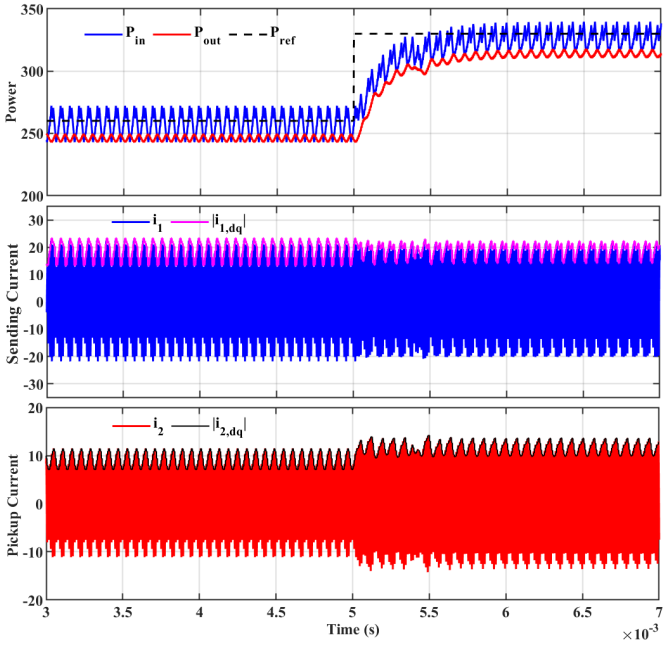

Fig. 8. Performance of the IPT system using the proposed FCS-MPC without damping term.

proximation in a dq synchronous reference frame. To validate the dynamic performance of the proposed control method in this reference frame, the dq-components of the sending/pickup currents (i.e., $i_{1,dq}, i_{2,dq}$) are shown in Fig. 8 and Fig. 9. As can be seen, the sending/pickup current amplitude in dq model (i.e., $|i_{dq}| = \sqrt{i_d^2 + i_q^2}$) can reach the steady-state condition very quickly about $0.1ms$ in the both case

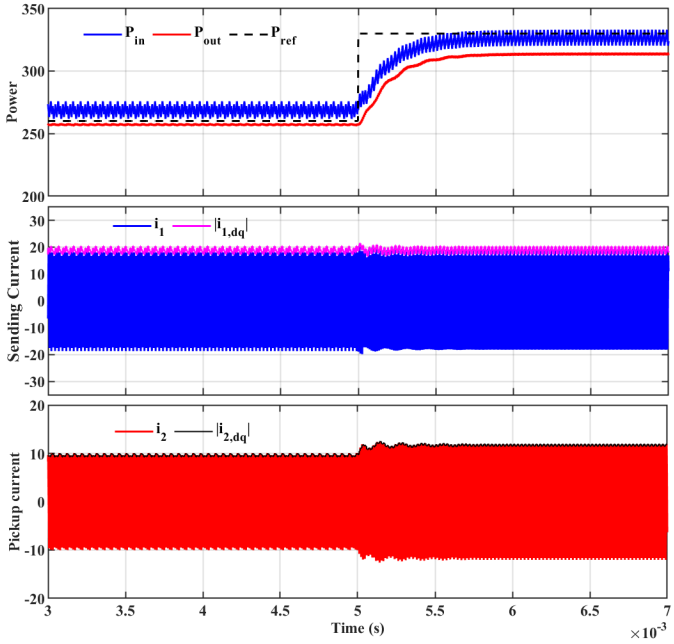

Fig. 9. Performance of the IPT system using the proposed FCS-MPC with damping term.

with/without damping term, while ensuring very low current fluctuation using the proposed FCS-MPC with the damping term. Therefore, the results in this case study verify that the proposed FCS-MPC strategy provides superior performance with a fast dynamic response, and eliminate current/power ripple.

V. Conclusion

The IPT systems with CVL can experience large oscillations in the sending/pickup current amplitude when using pulse skipping modulation strategies. To address this challenge an FCS-MPC is presented in this paper. In the process of control design a cost function with multiple control objectives is considered including the power tracking term and damping term. This method can inherently eliminate current/power ripples by predicting the future behaviour of the IPT system and determining the optimal switching state at each sampling time. Moreover, the proposed control method can achieve maximum power with fast dynamic response while ensuring soft switching operation. Simulation results confirm the effectiveness of the proposed FCS-MPC method.

References

[1] Ahmad, A., Alam, M. S., Chabaan, R. "A comprehensive review of wireless charging technologies for electric vehicles", *IEEE Trans. Transportation Electrification.*, vol. 4, no. 1, pp. 38-63, 2017.

[2] Feng, H., Tavakoli, R., Onar, O. C., Pantic, Z. "Advances in high-power wireless charging systems: Overview and design considerations", *IEEE Trans. Transportation Electrification.*, vol. 6, no. 3, pp. 886-919, 2020.

[3] G. Guidi, J. A. Suul, F. Jenset, and I. Sorfonn, "Wireless charging for ships: high-power inductive charging for battery electric and plug-in hybrid vessels," *IEEE Electr. Mag.*, vol. 5, no. 3, pp. 22–32, 2017.

[4] Y. Zhang, T. Lu, Z. Zhao, F. He, K. Chen, and L. Yuan, "Employing load coils for multiple loads of resonant wireless power transfer," *IEEE Trans. Power Electron.*, vol. 30, no. 11, pp. 6174–6181, Nov. 2015.

[5] T. Kan, T.-D. Nguyen, J. C. White, R. K. Malhan, and C. C. Mi, "A new integration method for an electric vehicle wireless charging system using LCC compensation topology: Analysis and design," *IEEE Trans. Power Electron.*, vol. 32, no. 2, pp. 1638–1650, Feb. 2017.

[6] G. Guidi and J. A. Suul, "Modelling techniques for designing high performance on-road dynamic charging systems for electric vehicles," *in Proc. 31st Int. Electric Vehicle Symposium and Exhibition Int Electric Vehicle Technology Conf.*, Sep. 2018, pp. 1–7.

[7] Y. Li, J. Hu, F. Chen, Z. Li, Z. He and R. Mai, "Dual-Phase-Shift Control Scheme with Current-Stress and Efficiency Optimization for Wireless Power Transfer Systems," *IEEE Trans. Circuits and Systems I: Regular Papers.*, vol. 65, no. 9, pp. 3110-3121, Sept. 2018.

[8] H. Li, J. Fang, S. Chen, K. Wang, and Y. Tang, "Pulse density modulation for maximum efficiency point tracking of wireless power transfer systems," *IEEE Trans. Power Electron.*, vol. 33, no. 6, pp. 5492–5501, Jun. 2018.

[9] W. Zhong and S. Y. R. Hui, "Maximum energy efficiency operation of series-series resonant wireless power transfer systems using on-off keying modulation," *IEEE Trans. Power Electron.*, vol. 33, no. 4, pp. 3595–3603, Apr. 2018.

[10] Zhou, J., Guidi, G., Ljøkelsøy, K., Suul, J. A. "Evaluation and Suppression of Oscillations in Inductive Power Transfer Systems With Constant Voltage Load and Pulse Skipping Modulation", *IEEE Trans. Power Electronics.*, 2023.

[11] Vazquez, S., Rodriguez, J., Rivera, M., Franquelo, L. G., Norambuena, M,. "Model predictive control for power converters and drives: Advances and trends", *IEEE Trans. Industrial Electronics.*, Vol. 64, no. 2, pp. 935-947, 2016.

[12] Karamanakos, P., Liegmann, E., Geyer, T., Kennel, R., "Model predictive control of power electronic systems: Methods, results, and challenges". *IEEE Open Journal of Industry Applications*, no.1, pp. 95-114, 2020.

[13] Qi, C., Lang, Z., Li, T. et al. "Finite-control-set model predictive control for magnetically coupled wireless power transfer systems", *Journal of Power Electron.*, vol. 21, no. 7, pp. 1095–1105, 2021.

[14] González-González, J. M., Triviño-Cabrera, A., Aguado, J. A. "Model predictive control to maximize the efficiency in EV wireless chargers", *IEEE Trans. Industrial Electronics.*, vol. 69, no. 2, pp. 1244-1253, 2022.

[15] Z. Karami, G. Guidi and J. A. Suul, "Continuous Control Set Model Predictive Control for Inductive Power Transfer system with Constant Voltage Load", accepted at *the 49th Annual Conference of the IEEE Industrial Electronics Society (IES).*, July, 2023, IECON, Marina Bay Sands Expo and Convention Centre, Singapore.

[16] Z. Karami, J. Zhou, G. Guidi and J. A. Suul, "Finite-Control-Set Model Predictive Control for Inductive Power Transfer Charging EV systems with Constant Voltage Load", presented at *the IEEE 11th International Conference of Power Electronic (ECCE).*, May 22-25, 2023, ICC,Jeju, Korea.

[17] Qi, Chen, et al. "Model predictive control for a bidirectional wireless power transfer system with maximum efficiency point tracking." *IEEE International Symposium on Predictive Control of Electrical Drives and Power Electronics (PRECEDE).* 2019.

[18] Y. Zhang, Z. Zhao, and K. Chen, "Frequency decrease analysis of resonant wireless power transfer," *IEEE Trans. Power Electron.*, vol. 29, no. 3, pp. 1058–1063, Mar. 2014.

[19] Y. He, Y. Tang, H. Xie, F. Wang, J. Rodriguez and R. Kennel, "Single-Phase H-Bridge Rectifier Fed High-Speed SRM System Based on Integrated Power Control," *IEEE Trans. Energy Conversion.*, vol. 38, no. 1, pp. 519-529, March 2023, doi: 10.1109/TEC.2022.3203626.

[20] P. Cortes, S. Kouro, B. L. Rocca, R. Vargas, J. Rodriguez, J. I. Leon, S. Vazquez, and L. G. Franquelo, "Guidelines for weighting factors design in model predictive control of power converters and drives," in *IEEE International Conference on Industrial Technology, ICIT* 2009., DOI 10.1109/ICIT.2009.4939742, Feb. 2009, pp. 1–7.